

Figure 2: Instructions per signal processing function under various data rates for a) SC-FDMA Demodulation, b) Subcarrier Demapper, c) Equalizer, d) Transform Decoder, e) Demodulation, f) Descrambler, g) Rate Matcher, h) Turbo Decoder, and i) Total Instructions.

Demapper (c_{r2}), Frequency Domain Equalizer (c_{r3}), Transform Decoder (c_{r4}), Constellation Demapper (c_{r5}), Descrambler (c_{r6}), Rate Matcher (c_{r7}) and Turbo Decoder (c_{r8}). As shown in Figure 1, these functions need to be executed in a specific order.

The main objective of this work is to identify the optimal GPP server where each function can be allocated so the total power consumption at the DC can be minimized satisfying, at the same time, the strict Quality of Service (QoS) constraints imposed by the CPRI protocol. To achieve this, we initially calculate - in terms of Total Instructions - the actual processing requirements of each baseband processing function under various wireless access system configurations. These calculations are carried out

using WiBench, an open source software implementation of the LTE protocol stack [2]. The processing requirements of each function are then used as input to a multistage ILP-based optimization framework that is able to assign each baseband sub-task to the suitable GPP in an energy efficient manner. Although the problem of BBU placement has been studied by several authors [4]-[7], the vast majority of these consider the BBU chain as a whole, without considering the specificities of its individual construction elements. In this study, however, it is shown that by i) *disaggregating* the softwarised BBU into a set of smaller sub-tasks, ii) *analyzing in depth the computational requirements* of each subtask and iii) *allocating* these subtasks to suitable GPPs as appropriate, significant benefits in terms of the operation efficiency of future 5G

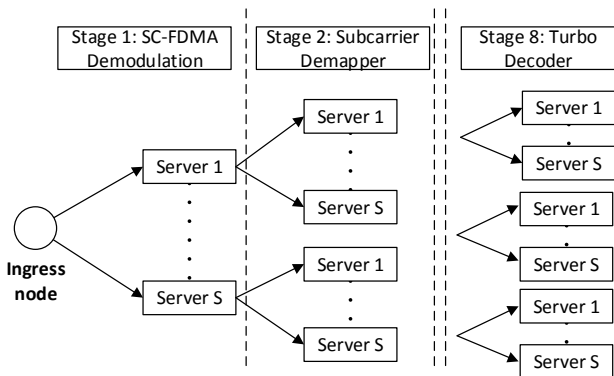


Figure. 3: Multi-stage optimization of disaggregated RAN functions

systems can be achieved. This study extends the state-of-the-art through:

- an extensive set of experiments used to characterize the processing requirements of the baseband functions as a function of the operational parameters of the wireless access network. These experiments led to the extraction of simple mathematical relations that can be used by network designers and operators to optimally allocate and size DC networks under various 5G network operational conditions.
- the development of an energy-aware multistage ILP-based optimization framework able to assign the BBU subtasks to a heterogeneous set of GPP elements reducing the DC power consumption by 20%.

III. BENCHMARKING FRAMEWORK

A. Experimental Platform Description

For our experiments we used WiBench, an open source suite for benchmarking wireless systems, and Intel's VTune Amplifier 2018, a performance profiler for software performance analysis. WiBench provides various signal processing kernels. These kernels are configurable and can be used to build applications to model wireless protocols. The LTE uplink that was used for the experiments, was provided by the WiBench suite and VTune was used to profile the LTE application. A summary of the functions that the BBU processing comprises is presented below. This includes:

- The Single Carrier - Frequency Diversity Multiple Access is a precoded Orthogonal Frequency Diversity Multiplexing (OFDM). It is preferred over OFDM, for the uplink transmission, because it is less susceptible to frequency offsets and has a lower Peak-to-Average Power Ratio. The SC-FDMA Demodulation function removes the Cyclic Prefix (CP) and performs N-point FFT.
- The Sub-carrier Demapper that extracts the data and the reference symbols from the subframes.
- The Frequency Domain Equalizer that estimates the Channel State Information (CSI) by the received pilot signal

through the Least Square estimation algorithm. It computes the channel coefficients, with the help of CSI, and equalizes the received data using as equalizer a zero forcing MIMO detector in the frequency domain.

- The Transform Decoder that performs M-point Inverse Fast Fourier Transfer (IFFT).
- The Constellation Demapper that receives the signal and extracts the binary stream by generating Logarithmic Likelihood Ratios (LLR).
- The Descrambler that descrambles the input sequence.
- The Rate Matcher that separates the input stream into R, where R is the Channel Code Rate, de-interleaves each code stream and removes redundant bits. For our experiments R was constantly set to 3.
- The Turbo Decoder that takes soft information for each code, in our case LLR, and it applies iterative the Soft-Input Soft-Output (SISO) algorithm. The Turbo Decoder consists of two SISO decoders that perform the trellis traversal algorithm, and one interleaver/deinterleaver. A higher number of iterations leads to a higher computation cost but achieves improved error correction performance. For all the experiments that were conducted the number of iterations was set to 5.

B. Main Results

To increase the statistical validity of the results produced by the profiler, a high number of iterations were performed (1000 subframes). The set of experiments we carried out was aiming at exploring the behavior of each processing function for different configurations of the LTE uplink system. In Figure. 2 we present the instructions performed, in order to process 1000 subframes, by each function as a function of the data rate for different modulation schemes.

Taking into consideration the variance of the measurements we can conclude that all functions present a linear dependence with the data rate. On the other hand, the influence of the modulation scheme, on the instructions number, differs for each function. More specifically we observe that the modulation scheme does not affect the instructions number for SC-FDMA Demodulation, Sub-carrier Demapper, Equalizer, and Transform Decoder. For the Constellation Demapper an exponential dependence of the modulation scheme is observed, while the Rate Matcher and the Turbo Decoder exhibit linear dependence.

We observe that the Turbo Decoder performs higher number of instructions, especially as the data rate increases, while the Constellation Demapper, the Rate Matcher and the Equalizer perform fewer instructions. This means that the Turbo Decoder, involving 1 to 4 orders of magnitude more instructions compared to other functions, determines by large the total number of instructions needed to process a subframe and how this number depends on the data rate and the modulation scheme.

TABLE 1: TECHNICAL SPECIFICATIONS OF THE SERVERS USED IN THE NUMERICAL EVALUATIONS

Enclosure (if applicable)	CPU Description	MHz	Chips	Cores	Total	RAM (GB)	Max IPS	Max Power (Watt)	Idle (Watt)	(IPS/watt)
QuantaGrid S31A-1U	Intel E3-1260L v5	2900	1	4	8	16	31802689	47.9	14.4	529836
QuantaGrid D51B-2U	Intel Xeon E5-2699 v4	2200	2	44	88	64	226542946	247	46.6	775056
QuantaGrid D52BQ-2U	Intel Xeon Platinum 8180	2500	2	56	112	192	378651974	426	39.5	833346
QuantaGrid T42S-2U	Intel Xeon Platinum 8176	2100	8	224	448	768	1304763025	1478	206	766748

IV. OPTIMIZATION OF SOFTWARED RAN FUNCTIONS

A. Problem formulation

Once the computational requirements $c_{ri}, i = 1, \dots, 8$, of the disaggregated RAN functions for RU $r \in \mathcal{R}$ have been determined (Figure. 2), a multi-stage ILP modeling framework able to assign the construction elements of the BBU chain to the suitable servers, is proposed. During stage 1, the first function of all fronthaul flows in the service chain (i.e., function SC-FDMA Demodulation) reaching the CU will be assigned to servers $s \in S$. This is achieved by minimizing the total compute resource power consumption, approximated through the following cost function:

$$f_1(\mathbf{x}_1) = \sum_{s \in S} \mathcal{E}_s \left(\sum_{r \in \mathcal{R}} x_{rs1} c_{r1} \right) \quad (1)$$

In (1), the summation $\sum_{r \in \mathcal{R}} x_{rs1} c_{r1}$ captures the total processing load of all c_{r1} functions processed at server s , x_{rs1} is a binary decision variable indicating whether function c_{r1} of RU $r \in \mathcal{R}$ is processed at server s or not, \mathbf{x}_1 is a vector containing all first stage decision variables x_{rs1} and \mathcal{E}_s is the power consumption model of server s .

Now let $Q_{\mathcal{R}1}$ be a set of paths for the FH flow of RU $r, r \in \mathcal{R}$ interconnecting the ingress node to server s , z_{rq} be the network capacity allocated to path $q \in Q_{\mathcal{R}1}$ for flow r and h_{r1} the transport network bandwidth requirements of function c_{r1} . h_{r1} can be directly estimated using the analysis [8]. (1) should be minimized subject to a set of network and processing demand constraints described through the following set of equations:

$$\sum_{s \in S} x_{rs1} = 1, \quad \forall r \in \mathcal{R} \quad (2)$$

$$\sum_{r \in \mathcal{R}} x_{rs1} c_{r1} \leq C_{s1}, \quad \forall s \in S \quad (3)$$

$$\sum_{s \in S} \sum_{q \in Q_{\mathcal{R}1}} x_{rs1} z_{rq} = h_{r1}, \quad \forall r \in \mathcal{R} \quad (4)$$

$$\sum_{r \in \mathcal{R}} \sum_{s \in S} \sum_{q \in Q_{\mathcal{R}1}} \delta_{rqe} z_{rq} \leq C_{e1}, \quad \forall e \in E \quad (5)$$

Constraint (2) limits the number of servers where c_{r1} -type of functions can be processed to one, (3) indicates that the total number of tasks that can be assigned to server $s, s \in S$ cannot exceed its available processing capacity C_{s1} at stage 1, while equations (4) - (5) introduce network demand and capacity constraints, respectively. In (5), δ_{rqe} is a binary coefficient

taking values equal to 1 if e belongs to path $q \in Q_{\mathcal{R}1}$ realizing demand $c_{r1}d$ at server s and C_{e1} is the available capacity of network link e at stage 1. After the solution of the first stage optimization problem, the remaining server and network capacity that can be used for the subsequent functions in the chain will be equal to:

$$C_{s1} - \sum_{r \in \mathcal{R}} x_{rs1} c_{r1} = C_{s2} \quad (6.1)$$

$$C_{e1} - \sum_{r \in \mathcal{R}} \sum_{s \in S} \sum_{q \in Q_{\mathcal{R}1}} \delta_{rqe} z_{rq} = C_{e2} \quad (6.2)$$

The decision variables x_{rs2} of the second stage optimization problem responsible to forward (through a set of candidate paths $q \in Q_{\mathcal{R}2}$) and allocate the second function of the FH service chain ($c_{r2} \equiv$ subcarrier demapper) to the optimal server s for processing, depends on the results of the first stage problem. Typical example includes the lists of paths $Q_{\mathcal{R}2}$ that can be used to forward the output of the first function in the chain to the subsequent one (i.e., c_{r1} to c_{r2}). This set depends on the decisions taken by the first stage problem regarding the servers where c_{r1} functions can be placed. Other examples include the available capacity at the servers and network links. All this unknown information captured through data vectors $\xi_t, t = 2, \dots, 8$, is revealed gradually as we proceed deeper in the processing of the service chain. The optimal compute resource assignment problem in disaggregated RAN environments can be solved through the minimization of the following nested cost function:

$$\min_{\mathbf{x}_1 \in \mathcal{X}_1} f_1(\mathbf{x}_1) + \mathbb{E} \left[\inf_{\mathbf{x}_2 \in \mathcal{X}_2(\mathbf{x}_1, \xi_2)} f_2(\mathbf{x}_2, \xi_2) + \mathbb{E} \left[\dots + \mathbb{E} \left[\inf_{\mathbf{x}_8 \in \mathcal{X}_8(\mathbf{x}_7, \xi_8)} f_8(\mathbf{x}_8, \xi_8) \right] \right] \right] \quad (7)$$

where extending (1) $f_t(\mathbf{x}_t, \xi_t) = \sum_{s \in S} \mathcal{E}_s (\sum_{r \in \mathcal{R}} x_{rst} c_{rt})$, $\xi_t = (C_{st}, C_{et}, h_{rt}, z_{rq})$ and based on (2)-(6) $\mathcal{X}_t, t = 2, \dots, 8$, can be described through:

$$\mathcal{X}_t := \left\{ \mathbf{x}_t : \sum_{s \in S} x_{rst} = 1, \sum_{r \in \mathcal{R}} x_{rst} c_{rt} \leq C_{st}, \sum_{s \in S} \sum_{q \in Q_{\mathcal{R}t}} x_{rst} z_{rq} = h_{rt}, \sum_{r \in \mathcal{R}} \sum_{s \in S} \sum_{q \in Q_{\mathcal{R}t}} \delta_{rqe} z_{rq} \leq C_{et}, C_{st-1} - \sum_{r \in \mathcal{R}} x_{rst-1} c_{rt-1} = C_{st}, C_{et-1} - \sum_{r \in \mathcal{R}} \sum_{s \in S} \sum_{q \in Q_{\mathcal{R}t-1}} \delta_{rqe} z_{rq} = C_{et} \right\}$$

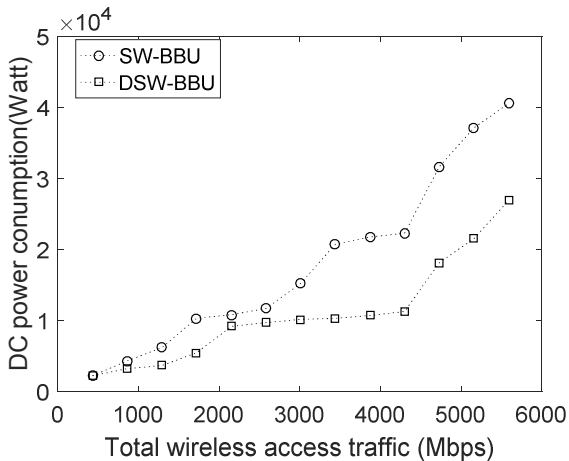


Figure 4: DC power consumption for the traditional softwareised BBU (SW-BBB) and the disaggregated SW-BBU (DSW-BBU) as a function of the total wireless access traffic.

The multi-stage linear programming model (7) can be decomposed into simpler sub-problems using the duality theory [9].

B. Numerical results

To quantify the benefits of the proposed Softwareised RAN approach, the simple DC network topology of Figure 1 is considered. This topology comprises 6 racks each one packed with 48 servers. Connectivity between racks is provided with the switching solution provided in [10]. In the numerical calculations we consider four types of servers, randomly placed inside the racks. The technical specifications of these servers is provided in Table 1, while their power consumption follows the linear stepwise function described in [11]. For the wireless access, we consider the topology described in [1] in which the served area is covered by a set of RRHs who forward their FH flows to the DCs for processing. Given that this study focuses on the computational aspects of the FH flows, we make the rational assumption that the transport network does not act as a bottleneck and, the same time, it has sufficient capacity to transfer all flows to the DCs for processing.

Figure 4 compares the performance of the proposed optimization scheme (denoted as Disaggregated Softwareised BBU – DSW-BBU) in terms of power consumption with the traditional Softwareised BBU (SW-BBU) as a function of the served traffic. As expected, the power consumption at the DCs increases with the wireless access load. However, the DSW-BBU offers much better performance due to its increased ability to mix and match compute and network resources, leading to improved utilization of the servers and to higher energy efficiency.

V. CONCLUSIONS

In this paper our experimental results show that there are specific functions (Turbo Decoder, Constellation Demapping, Rate Matcher and Frequency Domain Equalizer) at the LTE uplink that introduce much higher demands in terms of computational

resources. For these functions, the number of instructions executed has a linear dependence of the data rate. Since the baseband processing workload can be split into several functions, the allocation of each function to a suitable server using a purposely developed multistage optimization framework, in the scenario of a heterogeneous DC, can lead to better utilization of the servers and to higher energy efficiency.

ACKNOWLEDGEMENT

This work has been financially supported by the EU Horizon 2020 project 5G-PICTURE under grant agreement No 762057 and the EU Horizon 2020 project IN2DREAMS under grant agreement No 777596.

REFERENCES

- [1] A. Tzanakaki *et al.*, "Wireless-Optical Network Convergence: Enabling the 5G Architecture to Support Operational and End-User Services," in *IEEE Communications Magazine*, vol. 55, no. 10, pp. 184-192, OCTOBER 2017
- [2] Q. Zheng, Y. Chen, R. Dreslinski, C. Chakrabarti, A. Anastasopoulos, S. Mahlke, and T. Mudge, "WiBench: An Open Source Kernel Suite for Benchmarking Wireless Systems", 2013 IEEE International Symposium workload Characterization (IISWC), Portland, OR, 2013, pp.123-132.
- [3] S. Bhaumik, S. Preeth V/, M. Kashyap Jataprolu, G. Kumar, A. Muralidhar, P. Polakos, Vikram Srinivasan, and T. Woo. CloudIQ: a framework for processing base stations in a data center. In Proceedings of the 18th annual international conference on Mobile computing and networking (Mobicom '12). ACM, New York, NY, USA, 2012.
- [4] R. Riggio, D. Harutyunyan, A. Bradai, S. Kuklinski and T. Ahmed, "SWAN: Base-band units placement over reconfigurable wireless front-hauls," *2016 12th International Conference on Network and Service Management (CNSM)*, Montreal, QC, 2016, pp. 28-36.
- [5] F. Musumeci, C. Bellanzon, N. Carapellese, M. Tornatore, A. Pattavina, and S. Gosselin, "Optimal BBU Placement for 5G C-RAN Deployment Over WDM Aggregation Networks," *J. Lightwave Technol.* 34, 1963-1970 (2016)
- [6] D. Harutyunyan and R. Riggio. 2016. Functional Decomposition in 5G Networks. In *Proceedings of the 10th IFIP WG 6.6 International Conference on Management and Security in the Age of Hyperconnectivity - Volume 9701*, R. Badonnel, R. Koch, A. Pras, M. Drašar, and Burkhard Stiller (Eds.), Vol. 9701. Springer-Verlag New York, Inc., New York, NY, USA, 62-67
- [7] C. Colman-Meixner, G. B. Figueiredo, M. Fiorani, M. Tornatore and B. Mukherjee, "Resilient cloud network mapping with virtualized BBU placement for cloud-RAN," *2016 IEEE International Conference on Advanced Networks and Telecommunications Systems (ANTS)*, Bangalore, 2016, pp. 1-3.
- [8] U. Dötsch, U., M. Doll, H.-P. Mayer, F. Schaich, J., Segel, and P. Sehier, P. Quantitative Analysis of Split Base Station Processing and Determination of Advantageous Architectures for LTE. *Bell Labs Tech. J.*, 18: 105–128, 2013.
- [9] A. Shapiro, D. Dentcheva, A. Ruszczyński, *Lectures on Stochastic Programming: Modeling and Theory*, MOS-SIAM Series on Optimization, ISBN: 978-0-89871-687-0, 2009
- [10] J. Perelló *et al.*, "All-optical packet/circuit switching-based data center network for enhanced scalability, latency, and throughput," in *IEEE Network*, vol. 27, no. 6, pp. 14-22, November-December 2013.
- [11] A. Tzanakaki *et al.*, "Energy Efficiency in integrated IT and optical network infrastructures: The GEYSERS approach," *2011 IEEE Conference on Computer Communications Workshops (INFOCOM WKSHPs)*, Shanghai, 2011, pp. 343-348.